

Ion–Molecule Reactions: Theoretical Studies of the $[\text{N}_2 + \text{CO}]^+$ System

M. Hochlaf*

Theoretical Chemistry Group, University of Marne-La-Vallée,
Champs sur Marne, F-77454, Marne-la-Vallée, France

Received: March 5, 2004; In Final Form: March 31, 2004

Suitable one-dimensional cuts of the six-dimensional potential energy functions (PEFs) of the lowest electronic states of N_2CO^+ have been performed in order to elucidate the crucial role of this charge-transfer complex ion during the reactive processes involving N_2/N_2^+ and CO^+/CO . Specially, we are pointing out the importance of the vibronic couplings, the Renner-Teller interactions and the avoided crossings between these PEFs during these processes. These interactions are expected to mix all these electronic states, leading to the formation of atomic, diatomic, and triatomic species via the decomposition of the N_2CO^+ intermediate complex.

I. Introduction

Simple electrostatic attractions are not sufficient to explain the efficient reactive processes between N_2/N_2^+ and CO^+/CO , such as the efficient quenching of the CO^+ ($v^+ = 1$) ions by N_2 at 300 °K.¹ These reactions are viewed to involve the formation of the relatively strongly bound tetratomic charge-transfer complex N_2CO^+ .^{2–4} Such reactive processes may involve not only the potential energy surface of the electronic ground state of N_2CO^+ but also those of its electronic excited states. Recently, we have generated the six-dimensional potential energy function of the electronic ground state X^2A' of N_2CO^+ at the coupled cluster level of theory, and we have mapped the collinear potential energy curves of the lowest doublet excited states of N_2CO^+ correlating to the $\text{N}_2(X^1\Sigma_g^+) + \text{CO}^+(X^1\Sigma^+)$; $\text{N}_2^+(X^2\Sigma_g^+) + \text{CO}(X^1\Sigma^+)$; $\text{N}_2(X^1\Sigma_g^+) + \text{CO}^+(A^2\Pi)$; and $\text{N}_2^+(A^2\Pi_u) + \text{CO}(X^1\Sigma^+)$ asymptotes.⁵ In the vicinity of this work, we have also confirmed that the bonding in this ion is due to charge transfer from N_2 to CO^+ . The dissociation energy of the middle bond (D_0) is measured 0.7 ± 0.2 eV,³ while theoretical calculations at the Hartree–Fock and coupled cluster levels of theory give values such as 0.98 and 0.9 eV, respectively.^{5,6} The charge-transfer complexes, such as N_2CO^+ , have one common property—the parts of the potential energy function related to the diatom stretch coordinates differ strongly from the four-dimensional parts for the bending coordinates and the middle bond stretch, which are very shallow. These modes are expected to be coupled, and the charge-transfer complex can be considered as a four-dimensional van der Waals complex.

This work deals with studies of ion–molecule reactions involving N_2/N_2^+ and CO^+/CO . This type of reactions occurs in combustion systems, planetary atmospheres, cometary coma, and interstellar clouds where they play an important role in their chemistry.^{7–11} Such reactions are responsible for the formation of several triatomic species resulting in the decomposition of the tetratomic intermediate complex. Experimentally, the reactions between N_2/N_2^+ and CO^+/CO have been investigated at different collision energies, ranging from thermal to 40 eV.^{1,12} The reaction pathways are not well-known; however, it is commonly established that these reactions are related to dissociation mechanisms of the electronically excited N_2CO^{+*}

ion. Here, suitable one-dimensional cuts of the potential energy functions (PEFs) of the lowest electronic ground and excited states of N_2CO^+ of doublet multiplicity have been generated, allowing the elucidation of the reaction pathways between N_2/N_2^+ and CO^+/CO . Such studies will give an insight into the metastability of N_2CO^+ and on its role during such reactive processes.

II. Computational Methods

All electronic calculations have been carried out using the MOLPRO program suite.¹³ The generally contracted *spdf* cc-pVQZ basis set of Dunning has been used for N, C, and O atoms, resulting in 184 contracted Gaussian functions.¹⁴ The one-dimensional cuts of the PEFs of the doublet electronic states of N_2CO^+ have been generated using the complete active space self-consistent field (CASSCF) approach.¹⁵ To reduce the size of these calculations, the highest π and σ valence orbitals are not considered in the active space. However, all valence electrons were correlated, resulting in more than 50 000 Configurations State Functions (CSFs), in the C_s point group, to be treated. In these calculations, all electronic states have been averaged together. The accuracy of the relative energy position of the PEFs and of the dissociation limits computed in the present work is expected to be better than ~ 0.2 eV, which is high enough comparatively to the ± 0.4 eV error bars of the actual experimental determinations of the appearance energies of the products issued from the reactions between N_2/N_2^+ and CO^+/CO .

III. Results

In Figure 1 are depicted the one-dimensional cuts of the PEFs of the lowest electronic states of N_2CO^+ vs the middle stretch (R_{NC}), which is the most obvious reactive coordinate that one may consider when studying the $\text{N}_2/\text{N}_2^+ + \text{CO}^+/\text{CO}$ reactions. The electronic states presented in Figure 1 correlate to the $\text{N}_2(X^1\Sigma_g^+) + \text{CO}^+(X^2\Sigma^+)$, $\text{N}_2^+(X^2\Sigma_g^+) + \text{CO}(X^1\Sigma^+)$, $\text{N}_2(X^1\Sigma_g^+) + \text{CO}^+(A^2\Pi)$, and $\text{N}_2^+(A^2\Pi_u) + \text{CO}(X^1\Sigma^+)$ dissociation limits. The two lowest asymptotes have been positioned using the known D_0 value of $\text{N}_2\text{CO}^+(X^2A')$, the ionization potentials of N_2 and CO , and an appropriate thermochemical cycle. The third and the fourth limits are located using the known electronic excitation energies of CO^+ and N_2^+ , respectively. In Figure

* E-mail: hochlaf@univ-mlv.fr.

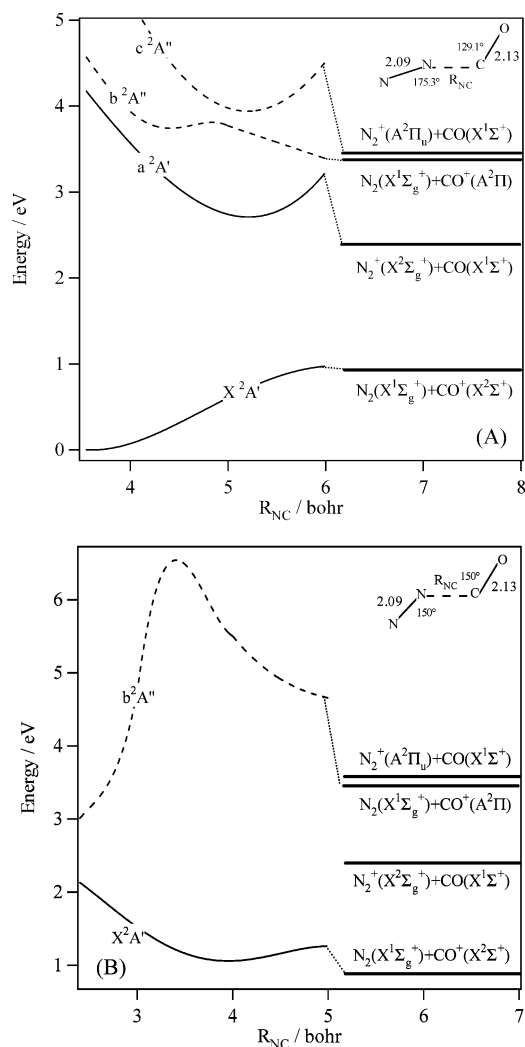


Figure 1. CASSCF potential energy curves of the lowest $2A'$ and $2A''$ electronic states of N_2CO^+ vs the middle stretch (R_{NC}). The other internal coordinates are fixed at their equilibrium values in $\text{N}_2\text{CO}^+(\text{X}^2\text{A}')$ (A) and for both in-plane angles ($\theta_1 = \theta_2$) set to $= 150^\circ$ (B).

In (A), the other internal coordinates are fixed at their equilibrium values in $\text{N}_2\text{CO}^+(\text{X}^2\text{A}')$, i.e., $R_{\text{NN}} = 2.09$, $R_{\text{CO}} = 2.13$ (in bohr); NNC angle (θ_1) = 175.3° and NCO angle (θ_2) = 129.1° ; and torsion angle (τ) = 180° .⁵ In Figure 1(B), both in-plane angles are fixed to 150° . These two figures show that the doublet states of N_2CO^+ exhibit avoided crossings—for instance, we can cite the one between the b^2A'' and c^2A'' states for $R_{\text{NC}} \sim 5$ bohr, which is responsible for the potential barrier in the lower electronic state and for the local minimum in the upper one (cf. Figure 1(A)). Additionally, the b^2A'' state presents a local minimum for short R_{NC} distance and for bent geometries (cf. Figures 1(A) and 1(B)). Moreover, since the reactions can occur through bent geometries of N_2CO^+ , we are presenting in Figure 2 the PEFs of these electronic states vs the bending angles. Figure 2(A) (Figure 2 (B)) is obtained by varying the NNC angle θ_1 (NCO angle θ_2) and by fixing the remaining internal coordinates at their equilibrium values in $\text{N}_2\text{CO}^+(\text{X}^2\text{A}')$. Figure 2(C) is obtained by varying symmetrically both in-plane angles and by fixing the middle bond (R_{NC}) to 2.4 bohr, which corresponds to the R_{NC} equilibrium distance at the local minimum of the 2Π state (cf. ref 5 for more details). The analysis of Figure 2(A) shows that the $\text{X}^2\text{A}'$ state has a small potential barrier to linearity ($\sim 8 \text{ cm}^{-1}$) vs the θ_1 angle responsible for its quasi-linear behavior already stressed out in our recent work

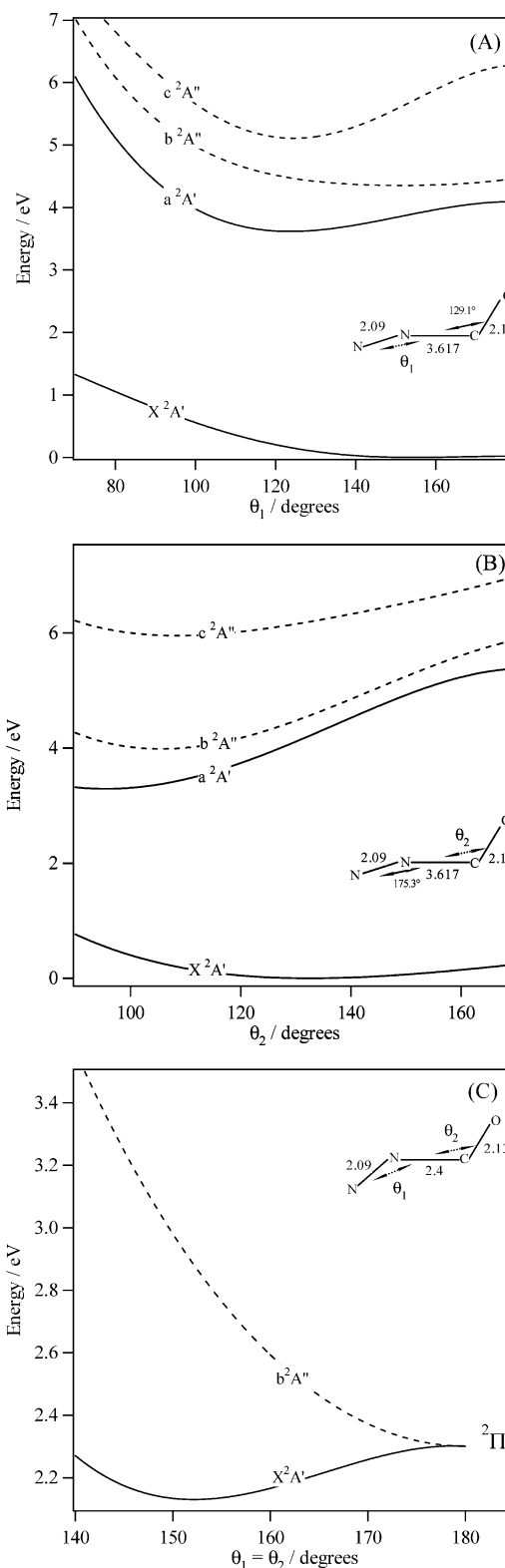


Figure 2. CASSCF one-dimensional cuts of the potential energy functions of the lowest $2A'$ and $2A''$ electronic states of N_2CO^+ vs θ_1 (A), θ_2 (B), and $\theta_1 = \theta_2$ (C). In (A) and (B) the distances are kept fixed at their equilibrium values in $\text{N}_2\text{CO}^+(\text{X}^2\text{A}')$. In (C), the R_{NC} distance = 2.4 bohr (see text for more details).

on the spectroscopy of $\text{N}_2\text{CO}^+(\text{X}^2\text{A}')$.⁵ For short R_{NC} distances, the b^2A'' state is expected to have a linear equilibrium geometry since its PEF goes up by bending both θ_1 and θ_2 angles (cf. Figure 2(C)). However, it presents a bent structure for longer R_{NC} distances (more than 3 bohr). The a^2A' and the c^2A'' states should have strongly bent structures with in-plane angles in the

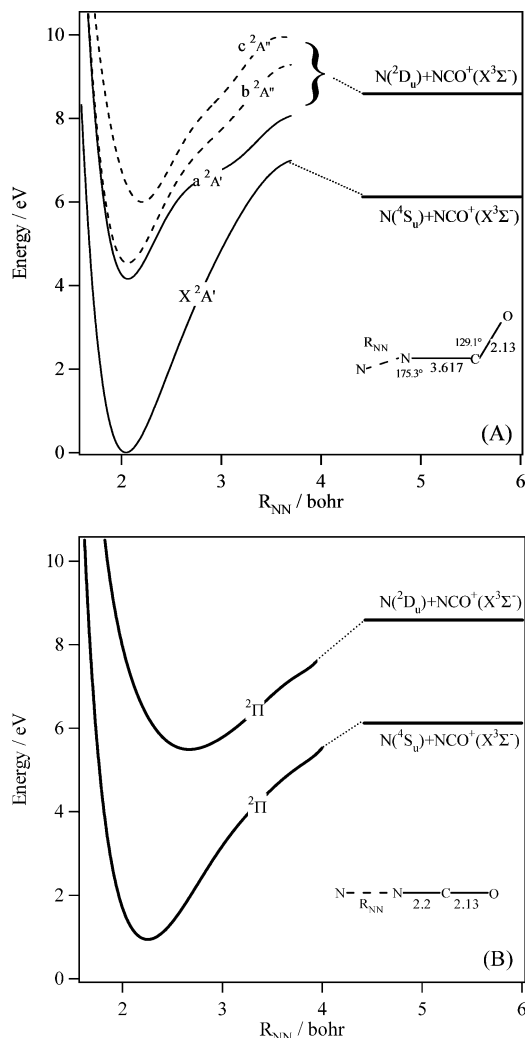


Figure 3. CASSCF one-dimensional cuts of the potential energy functions of the lowest $2A'$ and $2A''$ electronic states of N_2CO^+ vs R_{NN} . In (A), the other internal coordinates are kept fixed at their equilibrium values in $N_2CO^+(X^2A')$. In (B), the R_{NC} middle stretch is set to 2.2 bohr (\sim its equilibrium value in $NCO^+(X^3\Sigma^-)$) and for linear configurations.

range 100° – 130° . Additionally, Figure 2(C) shows that the X^2A' and b^2A'' electronic states correlate to the same 2Π state at linearity forming a linear/bent Renner-Teller system. Finally, we would like to point out that, according to the collinear one-dimensional cuts of the PEFs of the lowest doublet states of N_2CO^+ presented in ref 5, the 2Π state and the lowest $2\Sigma^+$ state (corresponding to the X^2A' state for bent geometries) form a conical intersection for $R_{NC} \sim 2.9$ bohr.

Lu et al.¹² have established, experimentally, that for collisional energies > 6 – 7 eV, the reactions between N_2/N_2^+ and CO/CO allow the formation of atomic and triatomic species resulting from the decomposition of the N_2CO^+ intermediate. To propose an insight into the reaction pathways undertaken there, we present in Figures 3 and 4 the evolution of the doublet electronic states of N_2CO^+ along the R_{NN} and R_{CO} stretches, respectively. Figure 3(A) depicts the one-dimensional cuts of the PEFs of the X^2A' , a^2A' , b^2A'' , and c^2A'' electronic states of N_2CO^+ vs the NN stretch (R_{NN}) and where the other internal coordinates are kept fixed at their equilibrium values in $N_2CO^+(X^2A')$. In Figure 3(B), we set the R_{NC} distance to 2.2 bohr (\sim its equilibrium value in $NCO^+(X^2\Pi)$) and the in-plane angles to 180° . At 2.2 bohr, only the two lowest 2Π states are expected to lie in the 0–10 eV internal energy region. Specially, the

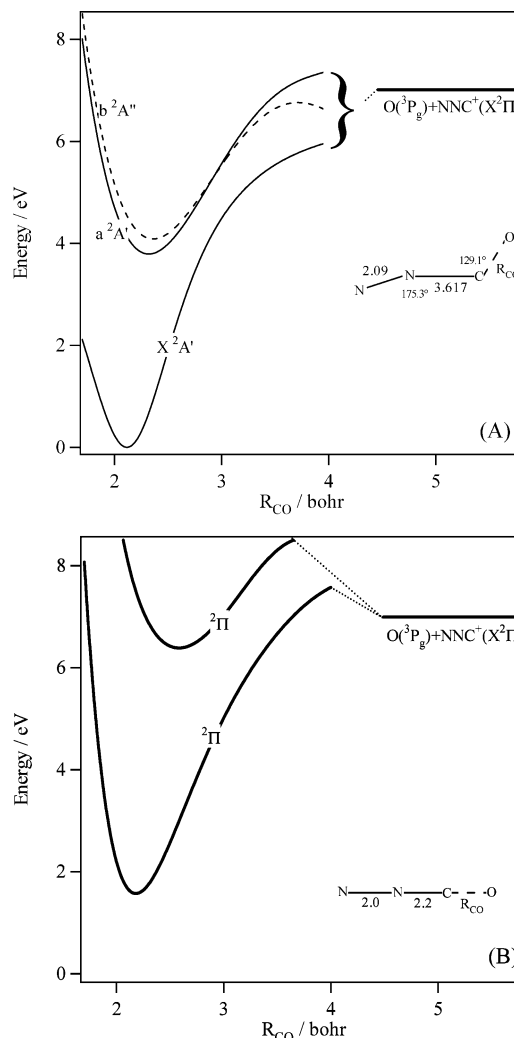


Figure 4. CASSCF potential energy curves of the lowest $2A'$ and $2A''$ electronic states of N_2CO^+ vs R_{CO} . In (A), the other internal coordinates are kept fixed at their equilibrium values in $N_2CO^+(X^2A')$. In (B), the R_{NC} middle stretch is set to 2.2 bohr (\sim its value in $CNN^+(X^2\Pi)$) and for linear configurations.

lowest $2\Sigma^+$ state is out of this range.⁵ The lowest asymptote $N(4S_u) + NCO^+(X^3\Sigma^-)$ is positioned using our CASSCF calculations. The NN bound dissociation energy D_e is calculated $\sim 6.2 \pm 0.1$ eV, which agrees well with the 6.0 ± 0.3 eV value, which can be deduced by combining the D_0 value of 0.7 ± 0.2 eV measured by Glosik et al.³ and the appearance energy of the NCO^+ fragment produced after reactions between N_2/N_2^+ and CO^+/CO in the Guided-Ion Beam experiment of Lu et al.¹² The multiple bound nature of the NN stretch may account for the relatively high dissociation energy found here for the breaking of this bound. Figure 3(A) shows that the two $2A'$ electronic states exhibit an avoided crossing for $R_{NN} \sim 3.5$ bohr, and that the a^2A' and b^2A'' states form a conical intersection for $R_{NN} \sim 1.8$ bohr. The two components of this conical intersection will form an avoided crossing for nonplanar geometries (C_1 point group) and may be coupled by the vibrational motions in the N_2CO^+ complex. Similarly, in Figures 4(A) and (B) are shown the one-dimensional cuts of the PEFs of the lowest doublet states of N_2CO^+ along the CO stretch (R_{CO}) for both bent planar (with $R_{NC} = 3.617$ bohr) and linear (with $R_{NC} = 2.2$ bohr) configurations, respectively. The $O(3P_g) + NNC^+(X^2\Pi)$ asymptote has been located using our CASSCF calculations. The D_e value for the CO bound in N_2CO^+ is calculated to be $\sim 7.0 \pm 0.1$ eV, which agrees with the $6.7 \pm$

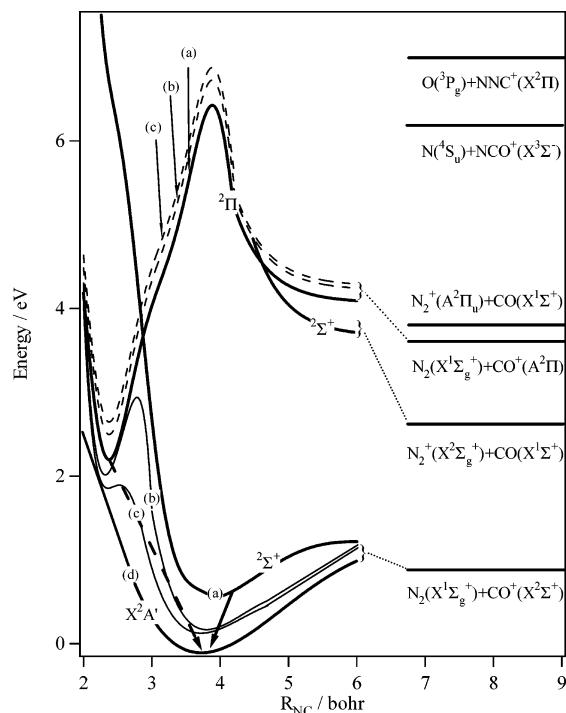


Figure 5. Energetic diagram showing the evolution of the lowest $2A'$ (solid line) and $2A''$ (dashed line) electronic states of N_2CO^+ vs R_{NC} for $\theta_1 = \theta_2 = 180^\circ$ (a), 160° (b), 140° (c), and 130° (d). R_{NN} and R_{CO} distances are fixed at 2.09 and 2.13 bohr, respectively, corresponding to their equilibrium value in $\text{N}_2\text{CO}^+(\text{X}^2\text{A}')$.

0.4 value obtained by adding the D_0 energy of the middle stretch in N_2CO^+ (0.7 ± 0.2 eV) and the CNN^+ appearance energy ($\sim 6.0 \pm 0.4$ eV) measured by Lu et al. in their $\text{CO}^+ + \text{N}_2 \rightarrow \text{O} + \text{CNN}^+$ reaction study.¹² Here again, the multiple bond nature of the CO stretch can be connected with this relatively high D_e value. One might note also the conical intersection occurring between the a^2A' and the b^2A'' states and the avoided crossing between the $\text{X}^2\text{A}'$ and a^2A' states for $R_{\text{CO}} \sim 3$ bohr.

The Renner-Teller and vibronic interactions, pointed out in this section, may couple the doublet electronic states of N_2CO^+ and they are expected to play a crucial role during the reactive processes between N_2/N_2^+ and CO^+/CO (see below).

IV. Discussion

The reactions between CO^+ and N_2 and between N_2^+ and CO have been investigated experimentally for different collision energies covering the range from thermal up to 40 eV.^{1,12} In addition to the initial reactants, the experimental results reveal the formation of the products issued from the charge transfer between the diatomics, and of the following species CNN^+ , NNO^+ , NCO^+ , C^+ , N^+ , and O^+ , proving the formation of the N_2CO^+ tetratomic intermediate complex and of its decomposition. Moreover, the $\text{CO}^+ + \text{N}_2$ and the $\text{N}_2^+ + \text{CO}$ reactions are found to give the same products in this collision energy range, suggesting that all the reactions proceed through the same N_2CO^+ intermediate, independently from the initial reactant charge-state.

Experimentally, the reactants can be prepared in their electronic ground states and/or with some internal energies corresponding to rotational and/or vibrational and/or electronic excitations. To help in understanding the reaction pathways we are presenting below, we show in Figure 5 a synthetic schematic diagram corresponding to the behavior of the lowest $2\Sigma^+$ and

2Π states along the middle stretch (R_{NC}) and for different bent structures. Specially, we are focusing on the evolution of the conical intersection between these two states. This diagram has been constructed using calculations similar to those shown in Figures 1, 2, 3, and 4. The results of these calculations are not presented here for clarity of the manuscript. According to Figure 5, several cases can be considered when N_2/N_2^+ and CO^+/CO are colliding together depending on the energy that the system contains initially. First, if the energy of the reactants is between 1 eV (threshold for $\text{N}_2 + \text{CO}^+$) and ~ 2.4 eV (threshold for $\text{N}_2^+ + \text{CO}$), this system has sufficient internal energy to form N_2CO^+ in its electronic ground state (cf. thick solid arrow in Figure 5), which can dissociate to produce $\text{N}_2 + \text{CO}^+$ in their electronic ground states. This reaction occurs through the six-dimensional potential energy surface of $\text{N}_2\text{CO}^+(\text{X}^2\text{A}')$, which correlates adiabatically to the first $2\Sigma^+$ state at linearity. Second, if the energy of the system is between ~ 2.4 eV and ~ 6.2 eV (corresponding to the appearance energy of the NCO^+ fragment), we can form $\text{N}_2^+ + \text{CO}$, in addition to the reaction pathway discussed above. Indeed, the reaction can take place via the avoided crossings and the conical intersections between the 2Π and $2\Sigma^+$ states; Figure 5 shows that if the N_2^+ ions collide with the CO molecules, the reaction follows the potential energy surface of the 2Π state, then its $2A'$ component interacts with the $2A'$ component of the first $2\Sigma^+$ at the conical intersection. The lowest $2A'$ component resulting from this interaction leads directly to the equilibrium geometry of $\text{N}_2\text{CO}^+(\text{X}^2\text{A}')$ (cf. the thick dashed arrow in Figure 5), which can dissociate later to $\text{N}_2 + \text{CO}^+$ and/or to $\text{N}_2^+ + \text{CO}$. Finally, if the energy of the reactant system is even higher than 6.2 eV, in addition to the products mentioned above, the reaction between the two diatomics produces the triatomic and atomic species formed from the decomposition of N_2CO^+ , as already observed in the experiments of Lu et al.¹² The final products may or may not have some internal energy.

Conclusions

The present calculations confirm that the dynamics of the N_2/N_2^+ and CO^+/CO reactions involve the formation of the tetratomic intermediate complex ion N_2CO^+ . We have pointed out the importance of the short-range internuclear distances during these processes. Specially, we have shown that the couplings between the electronic states of N_2CO^+ , including Renner-Teller couplings and conical interactions, play a crucial role during these reactions. For higher energies, electronic states of N_2CO^+ with higher spin multiplicities may exist allowing predissociation processes by spin-orbit couplings to take place. Such interactions mix the electronic states of N_2CO^+ correlating to the N_2/N_2^+ and CO^+/CO asymptotes. Finally and according to these calculations, electronically excited N_2CO^+ stable ions can be eventually found in the b^2A'' component of the 2Π state and for short R_{NC} distances.

Acknowledgment. The NERSC (UC Berkeley, USA) is thanked for computational time.

References and Notes

- (1) Hamilton, C. E.; Bierbaum, V. M.; Leone, S. R. *J. Chem. Phys.* **1985**, *83*, 601.
- (2) Ferguson, E. E.; Adams, N. G.; Smith, D. *Chem. Phys. Lett.* **1986**, *128*, 84.
- (3) Glosik, J.; Bano, G.; Ferguson, E. E.; Lindinger, W. *Int. J. Mass Spectrosc.* **1998**, *176*, 177.
- (4) Scott, G. B. I.; Fairley, D. A.; Freeman, C. G.; McEwan, M. J.; Anicich, V. G. *J. Chem. Phys.* **1998**, *109*, 9010.

- (5) Hochlaf, M.; Léonard, C.; Ferguson, E. E.; Rosmus, P.; Reinsch, E. A.; Carter, S.; Handy, N. C. *J. Chem. Phys.* **1999**, *111*, 4948.
- (6) Baker, J.; Buckingham, A. D. *J. Chem. Soc., Faraday Trans.* **1987**, *83*, 1609.
- (7) Anderson, W. R.; Vanderhoff, J. A.; Kotlar, A. J.; Dewilde, M. A.; Beyer, R. A. *J. Chem. Phys.* **1982**, *77*, 1677.
- (8) Perry, R. A. *J. Chem. Phys.* **1985**, *82*, 5485.
- (9) Anicich, V. G.; Huntress, W. T., Jr. *Astrophys. J. Suppl.* **1986**, *62*, 553.
- (10) Nejad, L. A. M.; Williams, D. A.; Charnley, S. B. *Mon. Not. R. Astron. Soc.* **1990**, *246*, 183.
- (11) Anicich, V. G. *Astrophys. J. Suppl.* **1993**, *84*, 215.
- (12) Lu, W.; Tosi, P.; Bassi, D. *J. Chem. Phys.* **2000**, *113*, 4132.
- (13) MOLPRO is a package of ab initio programs written by H. J. Werner and P. J. Knowles. Further details at www.tc.bham.ac.uk/molpro.
- (14) Dunning, T. H. *J. Chem. Phys.* **1989**, *90*, 1007.
- (15) Knowles, P. J.; Werner, H.-J. *Chem. Phys. Lett.* **1985**, *115*, 259.